Magnetic-field-induced suppression of tunnelling into a two-dimensional electron system

2002 J. Phys.: Condens. Matter 14 5561

(http://iopscience.iop.org/0953-8984/14/22/309)

INSTITUTE OF PHYSICS PUBLISHING JOURNAL OF PHYSICS: CONDENSED MATTER

J. Phys.: Condens. Matter **14** (2002) 5561–5574 PII: S0953-8984(02)34887-2

Magnetic-field-induced suppression of tunnelling into a two-dimensional electron system

T Reker[1], Y C Chung[1], H Im[1], P C Klipstein[1], R J Nicholas[1] and Hadas Shtrikman[2]

[1] Clarendon Laboratory, Department of Physics, University of Oxford, Parks Road, Oxford OX1 3PU, UK
[2] Braun Center for Submicron Research, Weizmann Institute of Science, Rehovot, Israel

Received 14 March 2002
Published 23 May 2002
Online at stacks.iop.org/JPhysCM/14/5561

Abstract

Tunnelling between a three-dimensional emitter contact and a two-dimensional electron system (2DES) is studied in magnetic fields aligned perpendicular to the barriers of a double-barrier heterostructure. The differential conductance around the Fermi energy exhibits a magnetic-field-dependent pseudogap. This pseudogap is shown to be thermally activated and to depend on the two-dimensional electron density. We attribute this pseudogap to an extra energy that an electron tunnelling from the emitter into the 2DES has to overcome as a result of the correlated state of the 2DES.

1. Introduction

Over the last decade a strong interest in the case of electrons tunnelling into a two-dimensional electron system (2DES) through a potential barrier has emerged. Since this technique gives information on the electronic spectral function, it was for instance used to determine the temperature dependence of the electron–electron scattering rate in clean two-dimensional systems [1]. Experiments on tunnelling between parallel 2DESs at high magnetic field applied perpendicular to the plane of the 2DESs gave evidence for intra-layer Coulomb correlations [2]. The magnetic field induced a pseudogap around the Fermi energy, i.e. a finite voltage was needed before any appreciable tunnelling current could flow between the parallel 2DESs and the tunnel current as a function of voltage exhibited a peak at finite bias.

Electrons in high magnetic fields behave as wavepackets whose size is set by the magnetic length $l_c = (\frac{\hbar}{eB})^{1/2}$. In two dimensions, the motion of these wavepackets in the plane of a 2DES is strongly correlated due to the remaining Coulomb interaction [2, 3]. When an additional electron tunnels into this correlated system, it creates a local 'uncorrelated' perturbation to which the system will react collectively in order to return to a correlated ground state. The width of the pseudogap is predicted to be determined by this energy difference between the initial uncorrelated and the final correlated state, presenting a tunnelling electron with an

additional energy barrier, which roughly corresponds to the electrostatic energy $e^2/4\pi\epsilon\langle a\rangle$, where $\langle a\rangle$ is the interelectron spacing in the 2DES [3]. Further, an activated behaviour of the conduction is predicted [3] with activation temperatures of typically $\sim$10 K, in good agreement with experiments [2] studying tunnelling between two parallel 2DESs (2D–2D) in perpendicular magnetic fields.

A magnetic-field-induced pseudogap was also found in tunnelling between a three-dimensional emitter and a 2DES (3D–2D) in high magnetic fields [5]. However, the experimental data were shown to be consistent with a linear density of states of the 2DES around the Fermi level. Accordingly, neither the activation of the pseudogap with temperature nor a dependence on two-dimensional electron density were found.

Varma *et al* [6] maintained that the pseudogap observed in the experiment by Eisenstein *et al* on 2D–2D magneto-tunnelling depends strictly on inter-layer correlations between the two parallel 2DESs and cannot be explained by single-layer correlations. It was thus claimed by these authors that the 'single-layer' 3D–2D experiment by Ashoori *et al* [5] does not show a true gap as in the case of the double-layer experiment. Eisenstein *et al* [2] speculate that the gap found in the single-layer system is disorder induced, whereas the gap observed in their double-layer experiments reflects the properties of a clean two-dimensional system. It is, however, argued that the effect even in their double-layer system is still a single-layer effect, and thus not dependent on inter-layer correlations.

In the remainder of this article, magneto-tunnelling data for electrons tunnelling from a three-dimensional emitter electrode into a 2DES in a quantum well subjected to a magnetic field parallel to the tunnelling direction will be presented and discussed. It will be shown that the tunnelling at energies close to the Fermi level is suppressed by the applied magnetic field. This will be explained in terms of a magnetic-field-induced suppression in the tunnelling density of states of the 2DES. A theoretical model introduced by Aleiner *et al* [7] will be shown to reproduce both the 2D–2D results by Eisenstein *et al* [2] as well as the experimental 3D–2D results obtained here. Disorder, although more prominent in the 3D–2D system studied here compared with 2D–2D structures, can be accommodated into this model.

Further, the pseudogap in the 3D–2D system studied will be shown to be temperature as well as density dependent. It can thereby be concluded that the effect is due to intra-layer correlations, showing that one is dealing with an inherently single-layer effect.

Moreover, it will be discussed whether the spin polarization of the 2DES, whose influence on tunnelling has so far been addressed mostly in theoretical studies [8–10], may play a role in the enhancement of the gap around the interesting region of filling factor $\nu = 1$, similar to the spin bottleneck for tunnelling of electrons observed by Chan *et al* [11].

2. Samples and method

Two symmetrical double-barrier heterostructures consisting of a 120 Å wide GaAs quantum well and 80 Å wide $Al_{0.28}Ga_{0.72}As$ barriers surrounded by $Al_xGa_{1-x}As$ contacts were grown on semi-insulating GaAs[001] substrates at the Weizmann Institute of Science. The nominal Al mole fractions in the contacts were $x = 0.05$ for sample I and $x = 0.06$ for sample II, respectively. The contact regions were n-type doped (Si) to a density of 2×10^{17} cm^{-3} and were separated from the double-barrier structure by 80 Å wide spacer layers. A self-consistent conduction band profile of sample I is shown in figure 1. The addition of a small mole fraction of Al in the contacts raises the conduction band edge and thus the Fermi energy in that region relative to the conduction band edge in the GaAs quantum well. This design results in the lowest sub-band in the well, E_1, falling energetically below the Fermi energy set by the doping density in the contacts. Electrons from the emitter will populate the first sub-band and a fixed

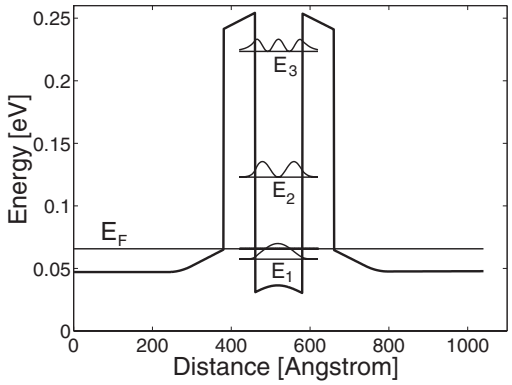

Figure 1. Self-consistently calculated conduction band profile (thick curve) for a $GaAs/Al_{0.28}Ga_{0.72}As/Al_{0.06}Ga_{0.94}As$ double-barrier heterostructure. E_F and $E_{1,2,3}$ denote the Fermi level and the quantized states, respectively.

electron density forms in the quantum well. By measuring the zero-bias conductance as a function of magnetic field, two-dimensional electron densities of $n_{2D} = 2.4 \times^{11}$ cm^{-2} for sample I and $3.2 \times^{11}$ cm^{-2} for sample II were obtained [12]. Besides the use of spacer layers, non-alloyed contacts were used, more than 7000 Å away from the double-barrier region, to reduce disorder in these structures. Although mobilities are not directly accessible for these structures, we estimate from previous growths of similar structures the mobilities to be at least of the order of $\mu \approx 100\,000$ cm^2 V^{-1}s^{-1}.

Circular mesas, 100 μm in diameter, were etched to include the double-barrier structure. Devices were subsequently bonded and current–voltage $I(V)$ measurements were performed on them at high magnetic fields and low temperatures. Two experimental set-ups were used; the first reached temperatures below 100 mK with magnetic fields up to $B = 12$ T. Temperature dependence measurements were carried out in a second system allowing measurements to be made at temperatures between $T = 1.5$ and 100 K in magnetic fields of up to 16 T.

3. Tunnelling in the presence of a magnetic field

3.1. Equilibrium conductance at the Fermi energy

The equilibrium conductance close to the Fermi energy at $T = 1.5$ K is shown in figure 2 for both samples. Landau levels (LLs) forming in the well are seen to push through the Fermi level with increasing magnetic field. The peaks in figure 2 have been labelled according to the above mentioned two-dimensional electron densities. Spin-splitting is only seen for the lowest LL. A slight increase in two-dimensional electron density with magnetic field is observable. The filling factor of $\nu = 1$ occurs at $B \approx 12$ and 16 T for samples I and II, respectively.

3.2. Current–voltage characteristics

Figure 3(a) shows the $I(V)$ characteristics for sample I at $B = 0$ T (bottom trace) as well as between $B = 4$ and 12 T in steps of 2 T. As can be seen from the trace at $B = 0$ T, the structure is resonant close to the bias origin, followed by a region of negative differential resistance (NDR) starting at about 30 mV. Applying a magnetic field parallel to the tunnelling current is seen to alter the $I(V)$ characteristics substantially.

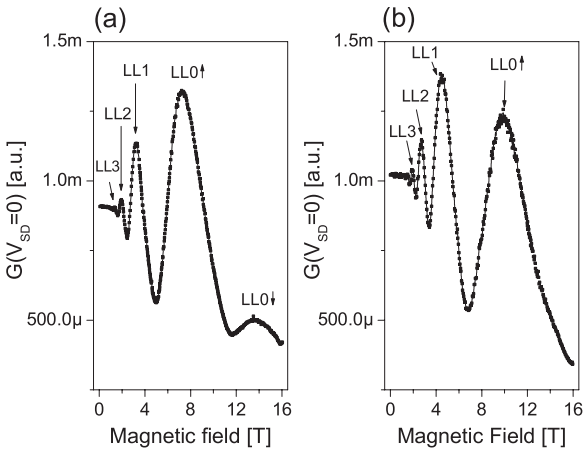

Figure 2. Equilibrium conductance at $T = 1.5$ K versus magnetic field (a) for sample I and (b) for sample II .

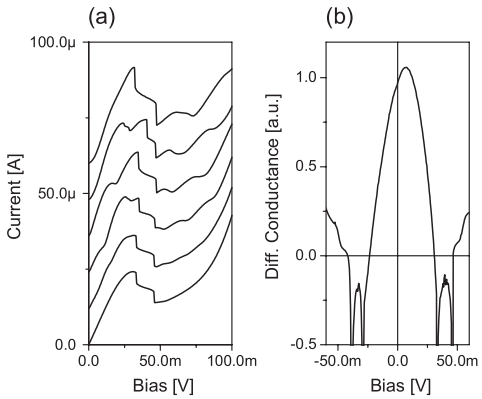

Figure 3. (a) $I(V)$ for a 100 μm device of sample I at magnetic fields of $B = 0$ (bottom trace), 4, 6, 8, 10 and 12 T (top trace) (offset along the positive ordinate for clarity) at $T = 100$ mK. (b) $G(V)$ around the origin for $B = 0$ T at $T = 100$ mK.

Additional features are clearly discernible at all finite fields. With increasing field, these additional features due to the LL quantization in the well become more pronounced and shift to higher voltages linearly in magnetic field [13]. Note that the features beyond the main resonance necessitate an inelastic process, which is most likely to be LO-phonon scattering in this case [14].

Looking closely at the current around the origin, one finds that apart from a modulation due to the LLs pushing through the Fermi level, a suppression of the current develops with increasing magnetic field (compare the curvature at the origin of the $I(V)$ traces at zero field with the one at 12 T). In the following sections, this suppression will be studied in non-equilibrium differential conductance $G(V)$.

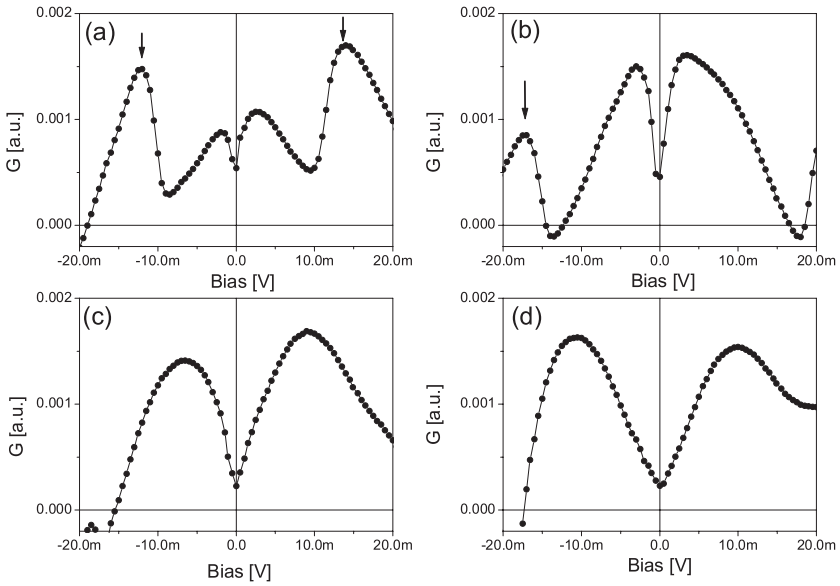

Figure 4. $G(V)$ for a 100 μm diameter mesa of sample I at $B = 6$, 8, 10 and 12 T at $T = 100$ mK. Arrows indicate features due to LL quantization.

3.3. Magnetic-field-induced features in the non-equilibrium conductance $G(V)$

Figure 3(b) shows the differential conductance $G(V)$ for the $I(V)$ trace at $B = 0$ T. A peak around zero bias is delimited on both sides by NDR regions. The slight asymmetry of the peak arises due to an asymmetry of the structure introduced during growth. It is worth mentioning that the broad peak in differential conductance does not reflect the width of the resonant state in the well alone, but rather a convolution of this width and the spectral width of the Fermi sea in the contacts, as will be discussed below.

The influence of a finite magnetic field on this peak in differential conductance is shown in figure 4. The differential conductance $G(V)$ traces of sample I, plotted for $B = 6$, 8, 10 and 12 T at $T \approx 100$ mK, reveal a suppression at the bias origin developing with magnetic field. The broad peak, which at $B = 0$ T was approximately centred around the bias origin, splits into two and moves out to finite biases with increasing B. The features marked by arrows are due to LL1 moving away from the Fermi level at the bias origin and are part of the general LL fan which allows the measured voltages to be converted into absolute energies. The voltage-to-energy conversion factor is thus determined from the fan plot to be $\alpha = 0.5$ meV mV^{-1}, reflecting the nearly symmetric nature of the structure.

Figure 5(a) shows the width of the suppression in differential conductance defined by the sum of the absolute peak biases, as seen in figure 4. As the data at low temperatures show, indicated by squares in figure 5(a), the suppression first becomes observable at fields just above $B = 1$ T, around $\nu \approx 8$. At even integral filling factors of $\nu = 2$, 4, 6 (indicated by arrows in the figure) the width 'diverges' and takes on values of the (much) larger cyclotron gap (values not included). This behaviour is as expected since at these filling factors all the states below the Fermi level are filled and all the states above it are empty. The pseudogap at these even integer filling factors is therefore expected to be determined by the cyclotron gap.

Following the $\nu = 4$, 2 cyclotron gap features in figure 5(a), plateaux form, extending up in field to $\nu \approx 2.5$ and 1.5, respectively. Above these filling factors there is an approximately linear increase with magnetic field until saturation occurs again at fields above $\nu = 1$.

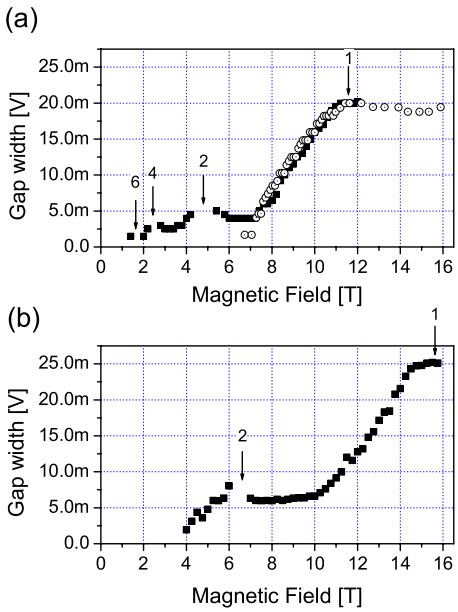

Figure 5. The peak to peak width of the conductance suppression around the bias origin (a) for sample I (squares, $T = 100$ mK; circles, 1.5 K) and (b) sample II (1.5 K). Arrows indicate integral filling factors corresponding to the minima in figure 2.

(This figure is in colour only in the electronic version)

The gap width in the plateau starting at $\nu = 1$ is about a factor of five larger than the gap width in the plateau following $\nu = 2$. This contrasts with a factor of approximately 1.5 in between the plateaux[3] following $\nu = 6$ and 4 as well as in between those following $\nu = 4$ and 2. This enhanced gap width could indicate a qualitative change of the gap in the spin-split LL regime compared with the spin-unresolved regime.

The measurement of the gap width for sample I was also carried out at $T = 1.5$ K up to $B = 16$ T. The data (open circles) have been added to the low-temperature data (squares) in figure 5(a). At this temperature, only the high-field features, seen at filling factors $\nu \leqslant 2$ in figure 5(a), are clearly observable. The gap width below $\nu = 1$ was seen to change very little up to the highest applied field, thus extending the low-temperature data in this respect up to 16 T.

A similar overall structure is observed in the data taken on sample II at $T = 1.5$ K, as shown in figure 5(b). However, the gap widths in the plateau regions are about 25% larger for sample II compared with sample I. This is attributable to the larger 2D electron density in sample II as will be explained in the next section. Note that the filling factor is not strictly linear in $1/B$, which implies a slight increase in carrier density with increasing magnetic field.

3.4. Temperature activation

Shown in figure 6(a) is the temperature dependence of the suppressed differential conductance $G(V)$ for sample II at $B = 16$ T between $T = 1.5$ K (squares) and 19.5 K (triangles), including several traces for temperatures in between, for example for $T = 7.53$ K (circles). Regions of positive and negative $\frac{\partial G}{\partial T}$ can be distinguished, separated by nodes showing almost

[3] The first gap width following the cyclotron gap at $\nu = 6$ has been taken as an indication for that 'plateau' value

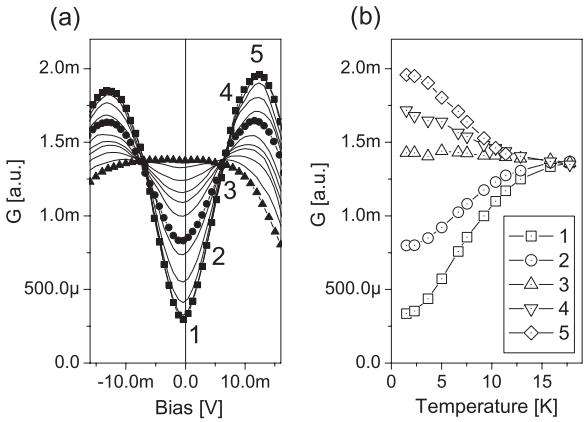

Figure 6. (a) The differential conductance $G(V)$ for sample II at $B = 16$ T for temperatures between $T = 1.5$ K (squares) and 19.5 K (triangles). (b) $G(T)$ at five different bias positions as marked in (a).

no temperature dependence. The explicit $G(T)$ dependence at the five voltages indicated in figure 6(a) is shown in figure 6(b). At voltage positions 1 and 2, $G(T)$ shows activated behaviour typical for insulating states. Position 3 acts as a separator, with positions 4 and 5 showing behaviour with temperature that is typical for metal-like states, i.e. a negative gradient $\frac{\partial G}{\partial T}$. Figure 6 gives additional strong evidence that a magnetic-field-induced pseudo-gap occurs around the Fermi level in these samples.

Plotting the differential conductance at the bias origin, $G(V = 0)$, in an Arrhenius plot for several magnetic fields (figure 7) reveals that the suppression is thermally activated in both samples. The saturation seen at low temperatures suggests a functional dependence of the data given by

$$f(T) = A\mathrm{e}^{-T_A/T} + B. \tag{1}$$

The dashed curves in figure 7(b), showing the fitted curves, are seen to reproduce the experimental data well. Similar fits were carried out on the data obtained for sample I.

Figure 8 shows the activation temperatures, T_A, extracted from these fits, plotted against magnetic field for both samples. Sample I (squares) shows an increase up to a maximum of $T_A \approx 9$ K close to $\nu = 1$ after which the activation temperature decreases again for even lower filling factors. Sample II (circles) shows a monotonic increase in activation temperature up to the highest field of 16 T, corresponding to $\nu \approx 1$.

As can be seen from figures 5 and 8, the activation temperature also becomes strongly enhanced in the spin-resolved regime $\nu \leqslant 2$, similar to the behaviour of the gap width. The maximum at $\nu = 1$ is particularly interesting, since the 2DES is known to be fully spin polarized and the in-plane conductivity is expected to be close to zero at this filling factor [4]. Moreover, the extracted activation energy at $\nu = 1$ of about 8.5 K is an order of magnitude smaller than the gap width energy[4] of about 60 K for the same sample at the same filling factor. The interpretation of these experimental results will be discussed below.

It is worth mentioning at this point that the ability to study tunnelling into both localized and delocalized states is an advantage that this 3D–2D system has to offer in comparison with 2D–2D systems, which rely on a finite in-plane conductivity to detect the tunnelling current between the two parallel layers.

[4] Extracted from figure 5(a) at $\nu = 1$ using the bias-energy-conversion factor to be discussed in the next section.

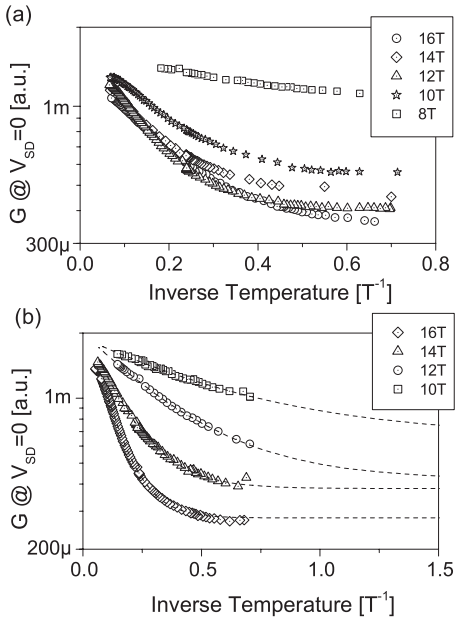

Figure 7. Arrhenius plots of the conductance at the bias origin for (a) sample I and (b) sample II.

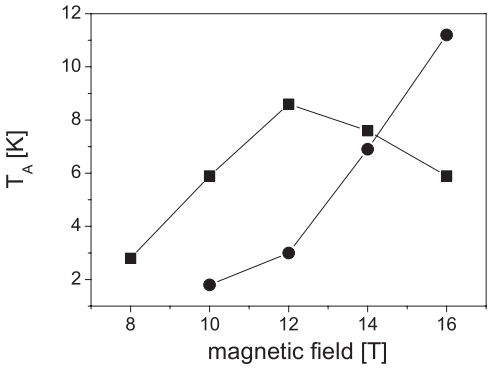

Figure 8. The activation temperatures for samples I (squares) and II (circles).

4. Discussion

4.1. A model describing tunnelling into a correlated 2DES

The tunnelling current, I, as a function of the applied voltage across the barrier, V, can be assumed to be of the form [15–17]

$$\mathrm{I}(V) \propto \int A_1(E)A_2(E - eV)[f(E, T) - f(E - eV, T)]\mathrm{d}E, \tag{2}$$

where $A_{1,2}$ denote the tunnelling density of states on the left and on the right of the barrier, respectively, and $f(E, T)$ stands for the Fermi distribution function.

Several models exist describing tunnelling into a 2DES in an applied magnetic field [3, 7, 15, 18]. It was suggested by Aleiner *et al* [7] that the tunnelling density of states close to

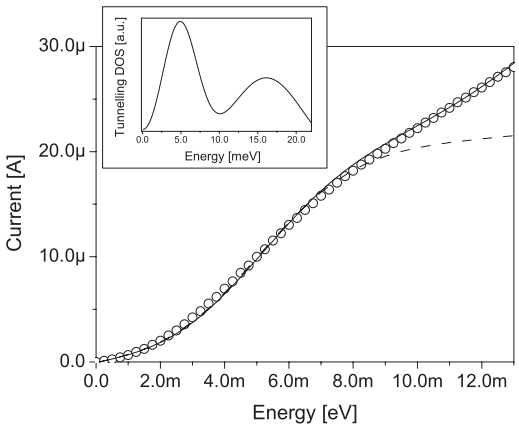

Figure 9. The current–energy characteristics of sample I at $T = 100$ mK and $B = 12$ T (open circles), as previously shown in figure 3, but now with a calibrated energy scale on the abscissa. The solid curve is obtained by the model discussed in the text, based on the two-dimensional DOS shown in the inset. The dashed curve represents a fit without the LL feature in the DOS.

the Fermi energy of a 2DES in a magnetic field can be described by two Gaussians at energies $\pm E_0$ relative to the Fermi level E_F,

$$A(E) \propto \frac{\hbar}{\sqrt{\Gamma}} \exp\left\{-\frac{(|E| - E_0)^2}{4\Gamma}\right\}, \tag{3}$$

where Γ is the width of the Gaussians. In the 'clean' limit of a homogeneous electron liquid, it was found that $\Gamma = E_0 k_B T$, whereas in the disorder-dominated regime (inhomogeneous electron liquid) $\Gamma = \text{const}$, where the constant reflects the disorder potential (k_B: Boltzmann's constant). In the 'clean' limit, the lower the temperature, the sharper the peaks in the density of states at $E = \pm E_0$. For the inhomogeneous case, a similar expression is found. In this case, the broadening of the peak is not caused by temperature-induced inhomogeneities but by disorder instead. Although initially derived for the low-B case, the tunnelling density of states, equation (3), was used by Turner *et al* [16] to successfully model data obtained on tunnelling between two 2DESs in high fields at $\nu \approx 0.5$: for a matched carrier density in both wells of $n_{1,2} = 0.97 \times 10^{11}$ cm^{-2}, a value of $E_0 = 2.6$ meV was determined. It is straightforward to see how a convolution of a double-Gaussian structure in equation (2) leads to peaks in $I(V)$ at $\pm 2E_0$, as observed in the 2D–2D tunnelling experiment by both Turner *et al* [16] as well as Eisenstein *et al* [2].

This ansatz will now be applied to the 3D–2D data presented in the last section. Shown in figure 9 (open circles) is the $I(V)$ trace of sample I at $B = 12$ T and $T = 100$ mK (figure 3), now with a calibrated energy scale on the abscissa. The inset gives the tunnelling density of states, A_2, assumed for the 2DES in the well[5]. It consists of two Gaussians centred at $E_0 = \pm 4.7$ meV relative to the Fermi level, of a width of $\Gamma = 1.7$ meV. A broadened feature in the DOS due to tunnelling into the first excited LL is introduced at $E_1 = 16$ meV. The origin of this LL feature can be seen in figure 3, where it defines the peak in the $I(V)$ trace at 12 T at about 32 mV.

[5] For simplicity, only the positive voltage axis is shown, due to the symmetry with respect to the bias origin, i.e. Fermi level.

Table 1. Dependence of the energies characterizing the magnetic-field-induced tunnelling suppression on two-dimensional electron density n_{2D}. E_{cond} was extracted from figure 5. E_0 denotes the energy obtained from fitting the model presented in section 4.1 to the experimental data. $E_C = \frac{e^2}{4\pi\epsilon\langle a_0\rangle}$ is the pure Coulomb energy set by the inter-electron distance $\langle a_0\rangle$. See text for further explanation.

Data	n_{2D} (10^{11} cm^{-2})	E_{cond} (meV)	E_0 (meV)	E_C (meV)
Eisenstein [2]	1.6	—	3.5	3.87
Sample I	2.4	5	4.7	4.78
Sample II	3.2	6.25	—	5.50

The density of states A_1 is taken to be the usual 3D-DOS

$$A_1(E) = 4\pi\left(\frac{2m^*}{h^2}\right)^{3/2}(E - E_{CB})^{1/2}, \tag{4}$$

where E_{CB} and m^* denote the conduction band edge and the effective mass in the emitter, respectively.

Using $A_{1,2}$ in equation (2), one obtains the full curve shown in figure 9, as a fit to the experimental data presented in the previous section, using the energy E_0 and the widths Γ of the Gaussians as parameters. The dashed curve, obtained by leaving the LL feature out of the tunnelling DOS, shows that the low-energy current is determined solely by the double-Gaussian DOS centred around the Fermi level. From this discussion, it becomes clear that due to a Fermi energy of almost 20 meV in the emitter in conjunction with the 3D-DOS, given by equation (4), the $I(V)$ characteristics do not show sharp peaks as in the 2D–2D case discussed above [2].

The fact that the same theoretical model, which has previously been used by Turner *et al* [16] to model the tunnelling suppression in a 'disordered' 2D–2D sample, can be applied to data obtained on a 'clean' 2D–2D sample by Eisenstein *et al* [2] as well as to the 3D–2D data presented here suggests that the fundamental cause of the magnetic-field-induced tunnelling gap must be of a similar nature in all three cases. Thus, neither the dimensionality of the emitter nor disorder appear to change the physical origin of the magnetic-field-induced tunnelling gap, which suggests that the observed pseudogap is effectively a single-layer effect.

4.2. Interpretation of the energy E_0 defining the gap width—its dependence on magnetic field and electron density

This section will focus on the interpretation of the energy E_0, defining the gap width, by looking at its dependence on magnetic field and on electron density. The results obtained for the samples studied here will be compared and contrasted with theoretical predictions and experimental findings by other groups.

4.2.1. Gap width dependence on two-dimensional electron density n_{2D}. Table 1 summarizes experimental results for the gap width obtained here and by Eisenstein's group [2] for filling factors $\nu \leqslant 1$ for different carrier densities. The third column gives the gap energy, E_{cond}, as extracted from half the measured gap width (measured from peak to peak) for $\nu < 1$ in differential conductance, as plotted in figure 5 and converted into (eV) using α. The fourth column lists the values for E_0, obtained by fitting Aleiner's DOS model to the measured $I(V)$ traces as above.

In this high-field regime, the gap width was seen to depend little on magnetic field. Since the high magnetic field localizes electrons on the scale of the magnetic length $l_c = \sqrt{\hbar/eB}$, it was argued by Eisenstein and co-workers [2,19] that the 2DES, although in the electron liquid regime, will be strongly correlated and at short distances will resemble a crystalline state. The minimum energy required to inject an additional electron into such a correlated electron liquid will be of the order of $E_C = \frac{e^2}{4\pi\epsilon\langle a_0\rangle}$, where the average inter-electron distance $\langle a_0\rangle$ is set by the densities n_{2D} through $\langle a_0\rangle = \frac{2}{\sqrt{\pi n_{2D}}}$, as defined in [2]. The respective values of E_C are also given in table 1 for comparison.

As can be seen, the measured gap energies in columns three and four increase with increasing electron density following the trend set by the values of E_C in column five. This supports the argument that the gap can be thought of as arising due to a difference in Madelung energy between an initial excited and uncorrelated state and a final relaxed and correlated two-dimensional state, as suggested by Eisenstein *et al* [2] and subsequently discussed in a more formal context by Johansson and Kinaret [3] and Haussmann [20]. Not only do the two samples studied here show tunnelling gaps very similar in magnitude to the experimental and theoretical results taken from the literature but they also fit into the trend set by these literature values which suggest a dependence on $\sqrt{n_{2D}}$.

Looking at experimental findings by other groups, Eisenstein *et al* [19] showed convincingly that the gap in a 2D–2D system in high magnetic fields ($\nu < 1$) is proportional to $\sqrt{n_{2D}}$. In contrast, in similar experiments on 2D–2D tunnelling in high magnetic fields by Brown *et al* [22], the gap was found to be independent of electron density in the wells over a wide range of filling factors $0.3 < \nu < 10$. A gap width independent of electron density has also been observed in a 3D–2D system by Ashoori *et al* [5].

To conclude, the clear density dependence of the gap width found here is in good qualitative and reasonable quantitative agreement with both experimental and theoretical studies performed on *clean* 2DESs.

4.2.2. Gap width dependence on magnetic field. At low magnetic fields B the dependence of the gap width on field shows more structure than predicted theoretically for both samples studied here (figure 5). In contrast, it was shown in the previous section that the high-field gap ($\nu < 1$) is rather insensitive to the magnetic field value and that it is of the order of the Coulomb interaction energy E_C.

It has been argued theoretically that the characteristic length determining the interaction energy in the high-field regime should be set by the magnetic length l_c rather than the inter-electron distance $\langle a_0\rangle$ [18]. This would make the gap proportional to $\sqrt{B}$. Two different theoretical approaches, however, predict a (low-field) gap approximately quadratic [7] in B or a gap approximately linear in B for high fields and quadratic for low fields [15]. Johansson's 'Wigner crystal' theory [3] predicts a crossover from a 'high-filling-factor' regime, where the magnetic field plays a role in determining the gap width through the magnetic length l_c, to a 'low-filling-factor' regime, in which the gap width saturates to a value determined by the inter-electron distance $\langle a_0\rangle$, once the magnetic field is high enough so that $\langle a_0\rangle \gg l_c$, which is typically the case for $\nu \leqslant 0.3$.

None of these predictions appear to apply to the data shown in figure 5, at least not over the entire range of magnetic fields. One could argue that, on a qualitative level, the observed linear increase starting at $\nu \approx 1.5$, and going over into a 'saturated' regime at $\nu \approx 1$, can be likened to the prediction of such a cross-over by Johansson *et al*, as mentioned above. However, the observed crossover occurs at much too high a filling factor of $\nu = 1$.

A similar behaviour to that seen here was, however, observed experimentally by Eisenstein *et al* [21]. Qualitative experimental evidence was given for a boundary to exist at $\nu \approx 1$ between two distinct tunnelling regimes, both of which support a tunnelling gap. Defining the half-width Γ as the peak position in $I(V)$ and thereby as the gap width E_0), Γ gradually rises with magnetic field from $B = 0$ to ∼4 T (corresponding to $\nu \sim 1.7$), where it abruptly begins to increase much more rapidly. By about $B = 6$ T ($\nu \sim 1$), this steep rise ends and a gentle increase resumes. A comparison with these data for $\nu \leqslant 2$ gives good qualitative agreement with the gap width dependence on magnetic field observed here. By contrast a linear increase with magnetic field was observed by both Turner *et al* [16] for a 2D–2D gap in differential conductance at fixed carrier density as well as fixed filling factor and by Ashoori *et al* [5] for the 3D–2D system. Such a 'simple' functional dependence is clearly not observed here.

The differences between the different sets of experimental results therefore lead us to conclude that the behaviour is strongly influenced by the level of disorder in the structures studied and we suggest that the behaviour which we report here is the low-disorder limit of the 3D–2D tunnelling.

4.3. Temperature dependence of the magnetic-field-induced gap

The magnetic-field-induced suppression of conductivity in the samples studied here shows a thermally activated behaviour with magnetic-field-dependent activation temperatures of the order of several kelvin (figure 8). Three salient features are worth pointing out.

Firstly, as seen for the gap width, the activation temperature becomes strongly enhanced in the spin-resolved regime $\nu \leqslant 2$. Secondly, the maximum at $\nu = 1$ is particularly interesting, since the 2DES is known to be fully spin polarized and the in-plane conductivity is expected to be (near) zero at this filling factor. Finally, the extracted activation energy at $\nu = 1$ of about 8.5 K is an order of magnitude smaller than the gap width energy of about 60 K for the same sample at the same filling factor. It is also worth mentioning again at this point that the experiments of both Eisenstein *et al* [19, 21] and Turner *et al* [16] on 2D–2D tunnelling in perpendicular magnetic fields cannot reliably measure the gap close to the integer (e.g. $\nu = 1$) or fractional quantum Hall states. This is because in their sample geometries the current tunnelling between the two 2DESs is detected by transport in the plane, which is greatly suppressed at these filling factors.

Figure 8 shows that for sample I a peak in activation temperature is observed at 12 T, which corresponds to $\nu \approx 1$. This could indicate that the spin polarization of the 2DES, which peaks at $\nu = 1$, plays a role in creating a spin bottleneck for tunnelling (as predicted by MacDonald *et al* [8]). Such a spin bottleneck was indeed observed in 3D–2D magneto-tunnelling by Chan *et al* [11]. These authors found a 'slow' tunnelling rate at $\nu = 1$ and reasoned that this suppressed rate was due to in-plane spin relaxation at a slow rate. Since this slow tunnelling rate was shown to arise only in spin-polarized quantum Hall states at temperatures lower than the Zeeman energy, the authors described it as arising due to a spin bottleneck in which in-plane relaxation must proceed before additional electrons can tunnel into the system. In this context, Palacios and Fertig [10] predicted that at $\nu \approx 1$ the signature of skyrmions in the $I(V)$ characteristics should be observable as a suppression of the tunnelling current near the Fermi level surrounded by peaks at finite biases.

This spin-bottleneck mechanism could thus explain the peak and the strong enhancement of the activation temperature around $\nu = 1$. The activation temperature of about 9 K at $\nu = 1$ implies an enhancement by a factor of approximately ten relative to (half) the single-particle bare Zeeman energy at this field, in rough agreement with what was found experimentally for a single 2DES [23].

The difference between the energy scales of the activation and the gap energies by approximately one order of magnitude, as observed here, agrees with what was predicted theoretically [3,20] and shown experimentally [2,5,16]. A straightforward explanation was given: an electron tunnelling into a correlated 2DES creates an uncorrelated 'defect' in the 2DES. The system relaxes to its ground state by emitting characteristic collective excitations. This creates a pseudogap for tunnelling of electrons of the order of the Coulomb interaction energy. This pseudogap exhibits thermally activated behaviour caused by thermally excited collective excitations. The activation temperatures, however, are not determined by the gap energy but rather by the (much lower) characteristic energy of the collective excitations of the system [20].

Around filling factor $\nu = 1$, the relevant collective excitations are likely to be spin related: for a perfectly uniform two-dimensional system precisely in the $\nu = 1$ spin-polarized state, tunnelling injects a minority spin. Since this is not the lowest-energy excitation, over time the two-dimensional system can lower its energy by flipping more spins to create skyrmions. Since the energy of the two-dimensional system is lowered, more electrons can tunnel from the three-dimensional emitter electrode. When the timescale for spin relaxation is long, the intermediate stage forms a bottleneck and temporarily prevents electrons from tunnelling [8,11].

The results obtained here for the temperature dependence of the conductance may also help to resolve the dispute about the influence of disorder on the gap. Looking at the Arrhenius plots, figure 7, an activated behaviour of the equilibrium conductance for temperatures below about 10 K is observed. For the lowest temperatures, however, the conductance saturates at a finite value. Within Aleiner's model, used above to model the experimental data obtained here and by Eisenstein *et al* [19], the magnetic-field-induced gap in $I(V)$ arises due to a gap in the electronic spectral function at the Fermi energy, surrounded by two peaks. The width of these peaks is proportional to temperature for a homogeneous correlated electron liquid, whereas for an inhomogeneous (disorder-dominated) liquid this width is independent of temperature and determined by disorder [7]. The temperature-dependent width for the homogeneous liquid leads to a thermally activated equilibrium conductance [16]. A temperature-independent width, however, will lead to a constant, saturated conductance. It could therefore be speculated that the data shown in figure 7 show both behaviours—the activated behaviour of a clean two-dimensional system at high temperatures and the saturated conductance at the lowest temperatures, once the temperature becomes comparable to the disorder potential.

Comparing these experimental findings with those obtained by other groups, Eisenstein *et al* [2] observed activated behaviour of a magnetic-field-induced 2D–2D tunnelling suppression in the high-field regime for $\nu \leqslant 2$ with activation temperatures of up to $T = 5$ K in the upper spin branch and up to 10 K in the lower spin branch of the lowest LL. However, no monotonic dependence on ν (or B) was found and the geometry of their samples prevented them from obtaining data in the interesting region around $\nu = 1$. Thus, no comparison with figure 8 can be drawn other than that the order of magnitude of the activation temperatures found here agrees well with those reported by Eisenstein *et al* [2]. Turner *et al* [16,22] also studied the temperature dependence of the conductance in a 2D–2D system extensively, and activated behaviour was found. The order of magnitude of the activation temperatures and the qualitative form of $G(V)$ on temperature are similar to that obtained here. In contrast Ashoori *et al* [5] observed a non-activated but temperature-dependent conductance. This is, in fact, as expected since a linear density of states around the Fermi level, as observed in their experiments, should not give activated behaviour.

Thus, the activated behaviour which we observe in our 3D–2D tunnelling as well as the values of the activation temperatures found here are in agreement with what was observed experimentally in 2D–2D tunnelling studies [2, 16] and predicted theoretically assuming a Coulomb-correlated 2DES [3,20]. The enhancement and peak in activation temperature found

here around $\nu = 1$ may suggest that slow in-plane spin relaxation creates a bottleneck for tunnelling of electrons.

5. Conclusion

Tunnelling between a three-dimensional emitter contact and a 2DES has been studied in magnetic fields aligned perpendicular to the barriers of a double-barrier heterostructure. Apart from the well known LL features, the differential conductance around the Fermi energy was shown to exhibit a magnetic-field-dependent pseudogap. The pseudogap was studied as a function of magnetic field, two-dimensional electron density and temperature.

The results can be fitted well by modelling the tunnelling DOS of a 2DES in an applied magnetic field [7]. Together with the observed dependence of the pseudogap on two-dimensional electron density and the thermally activated behaviour of the conductance, this suggests that the effect is essentially a single-layer phenomenon, in agreement with recent findings presented by Spielman *et al* [24]. The peculiar behaviour of the pseudogap around filling factor $\nu = 1$ provides some evidence for the existence of a spin bottleneck for tunnelling electrons.

Acknowledgments

This work was funded by the Engineering and Physical Sciences Research Council (EPSRC). TR gratefully acknowledges further financial support by the Friedrich Flick Stiftung and the European Commission's Large Scale Facility programme (HPRI-CT-1999-00069). TR also wishes to thank Moty Heiblum, Ady Stern and Markus Kasner for helpful discussions.

References

[1] Murphy S Q, Eisenstein J P, Pfeiffer L N and West K W 1995 *Phys. Rev.* B **52** 14 825
[2] Eisenstein J P, Pfeiffer L N and West K W 1992 *Phys. Rev. Lett.* **69** 3804
[3] Johansson P and Kinaret J M 1994 *Phys. Rev.* B **50** 4671
Johansson P and Kinaret J M 1993 *Phys. Rev. Lett.* **71** 1435
[4] Chakraborty T and Pietilainen P 1995 *The Quantum Hall Effects: Integral and Fractional* (New York: Springer)
[5] Ashoori R C, Lebens J A, Bigelow N P and Silsbee R H 1990 *Phys. Rev. Lett.* **64** 681
[6] Varma C M, Larkin A I and Abrahams E 1994 *Phys. Rev.* B **49** 13 999
[7] Aleiner I L, Baranger H U and Glazman L I 1995 *Phys. Rev. Lett.* **74** 3435
[8] MacDonald A H 1999 *Phys. Rev. Lett.* **83** 3262
[9] Kasner M, Palacios J J and MacDonald A H 2000 *Phys. Rev.* B **62** 2640
[10] Palacios J J and Fertig H A 1997 *Phys. Rev. Lett.* **79** 471
[11] Chan H B, Glicofridis P I, Ashoori R C and Melloch M R 1999 *Phys. Rev. Lett.* **83** 3258
[12] Leadbeater M L, Eaves L, Simmonds P E, Toombs G A, Sheard F W, Claxton P A, Hill G and Pate M A 1988 *Solid State Electron.* **31** 707
[13] Mendez E E, Esaki L and Wang W I 1986 *Phys. Rev.* B **33** 2893
[14] Leadbeater M L, Alves E S, Eaves L, Henini M, Hughes O H, Celeste A C, Portal J C, Hill G and Pate M A 1989 *Phys. Rev.* B **39** 3438
[15] Fogler M M, Koulakov A A and Shklovskii B I 1996 *Phys. Rev.* B **54** 1853
[16] Turner N, Nicholls J T, Linfield E H, Brown K M, Jones G A C and Ritchie D A 1996 *Phys. Rev.* B **54** 10 614
[17] Shrieffer J R, Scalapino D J and Wilkins J W 1963 *Phys. Rev. Lett.* **10** 336
[18] He S, Platzman P M and Halperin B I 1993 *Phys. Rev. Lett.* **71** 777
[19] Eisenstein J P, Pfeiffer L N and West K W 1995 *Phys. Rev. Lett.* **74** 1419
[20] Haussmann R 1996 *Phys. Rev.* B **53** 7357
[21] Eisenstein J P, Pfeiffer L N and West K W 1994 *Surf. Sci.* **305**
[22] Brown K M, Turner N, Nicholls J T, Linfield E H, Pepper M, Ritchie D A and Jones G A C 1994 *Phys. Rev.* B **50** 15 465
[23] Nicholas R J, Haug R J, von Klitzing K and Weimann G 1988 *Phys. Rev.* B **37** 1294
[24] Spielman I B, Eisenstein J P, Pfeiffer L N and West K W 2000 *Phys. Rev. Lett.* **84** 5808